Tutorial: Incorporating near-surface velocity anomalies in pre-stack depth migration models

Ian F. Jones[1*]

Abstract

Unresolved velocity anomalies in the near surface degrade deeper imaging. As a consequence, great care needs to be taken to ensure that all significant near-surface effects have been dealt with before attempting to build the deeper parts of a velocity–depth model. In order to incorporate velocity anomalies into the model, a range of options can be used, depending on whether the geobody geometry alone is discernible, or whether its velocity distribution is also known. Here I describe current industrial practice for building complex near-surface models, which is based on a range of approximate techniques, as well as the more complete solution offered by the emerging technology of waveform inversion. Although building complex near-surface models is a painstaking process, a suitable near-surface velocity model can usually be obtained.

Introduction

Compensating for near-surface small-scale velocity anomalies is a difficult and demanding task, and is usually dealt with very approximately (e.g., Armstrong, 2001; Armstrong et al., 2001; Jones, 2010). Here I review several methods, both for shallow marine environments where we have limited fold, and for deep water where the useable fold will be higher. Land environments are also mentioned because they add further complexity to the near-surface problem. In addition, I describe the emerging technology of waveform inversion, its limitations, and what we hope to achieve with it. This analysis is in the context of building velocity-depth models for 3D pre-stack depth migration (PreSDM), but I do not address the specific limitations of individual migration algorithms, other than to mention some scale-length assumptions made by ray-based methods.

All raypaths that pass through a near-surface velocity anomaly will be affected by it, distorting the subsurface response over a distance of about half a cable length to either side of the anomaly. The distorted region actually extends beyond half a cable length due to the influence of the Fresnel zone, because we are really dealing with wavefronts rather than hypothetical rays. In addition, conventional velocity analysis and time processing deals with all traces in a common midpoint (CMP) gather using the same 1D velocity function; hence conventional time processing cannot compensate for these effects.

In this review, by 'near surface' I refer to features whose fold of coverage in common reflection point (CRP) gathers is either too low or near the practical limit for autopickers to be able to determine residual moveout, and/or whose lateral extent is too small for ray-based methods to perform reliably, i.e., features with lateral velocity changes occurring over distances less than several times the dominant wavelength of the seismic wavefronts reflected from them.

The nature of the problem is perhaps best outlined with some simple synthetic modelling. Figure 1 shows the interval velocity profile for a relatively simple model with almost flat-lying geology, but with a near-surface channel filled with low-velocity sediment. To assess the behaviour of the modelled data, we first look at unmigrated offset planes, following normal moveout (NMO) correction, and then progress to the behaviour of the data following migration with various velocity models. Figure 2 shows the individual

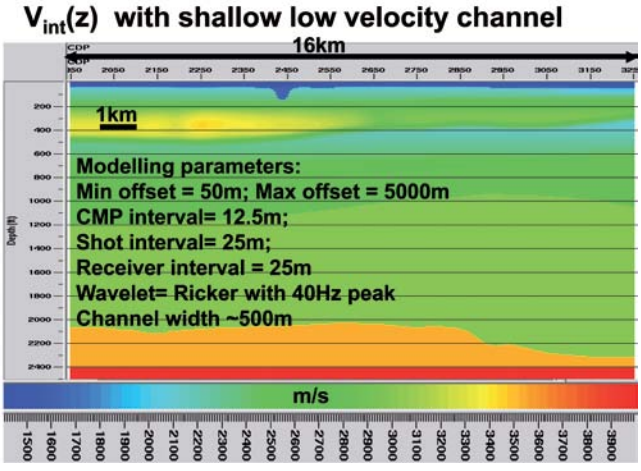

Figure 1 *Velocity-depth model for synthetic data, based on a North Sea case study.*

[1] *ION GX Technology, 1st Floor, Integra House, Vicarage Road, Egham, Surrey TW20 9JZ, UK.*
[*] *Corresponding author, E-mail: Ian.Jones@iongeo.com*

offset planes for 50 m, 1050 m, and 3550 m after NMO correction with a sparse smooth velocity function picked manually from the data, and hence not containing any details of the channel feature. The upper parts of the sections have been muted to remove moveout stretch of primary and refraction events. The CMP gather on the right of the figures shows optimally flattened events, as picked in the manual velocity analysis.

It should be noted that both NMO-corrected and pre-stack time migrated (PreSTM) data, even with the 'correct' velocity model, will exhibit the push-down distortion, as neither can correctly deal with the velocity anomaly of short spatial wavelength. In other words, both NMO and PreSTM make the assumption that all traces in a CMP gather should be processed with the same 1D velocity-time function pertaining to that CMP location. The actual velocity function may change laterally, but at any given CMP, traces from all offsets in the gather are treated as if they propagated in the same laterally invariant velocity-time field.

Kirchhoff PreSDM using the correct velocity model produces a good image (Figure 3a). Note that this is not the manually picked smooth velocity model, but rather the model used to create the synthetic data, which contains the details of the channel feature. This result demonstrates that PreSDM with an appropriate velocity model is capable of removing raypath distortion. However, using a velocity model derived from Dix inversion of root mean square (RMS) velocities for migration, such as would have been picked using conventional velocity analysis, without the

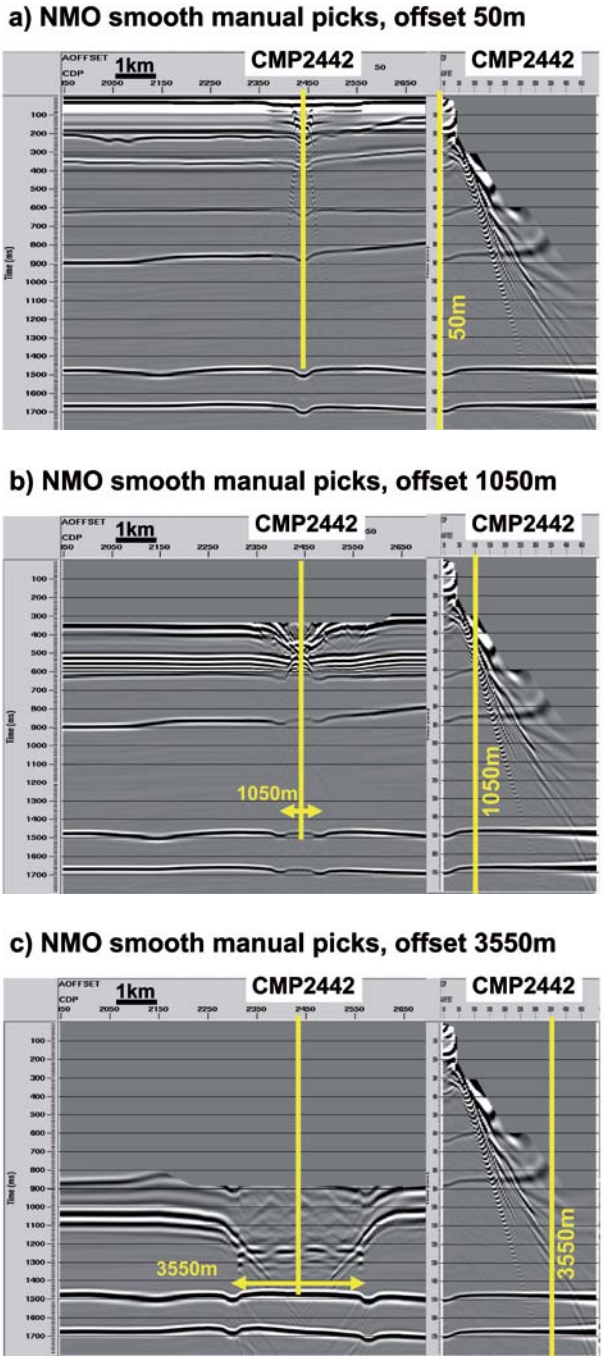

Figure 2 (a) Near, (b) mid, and (c) far-offset sections from the data after NMO with a smooth manually picked velocity function. Distortion due to the channel persists to each side of the channel over a distance of more than half the offset used. On the right is a CMP gather from the centre of the channel (maximum offset 5 km), showing the push-down on the near traces. The linear dipping 'noise' events in the gather are the direct wave and various refractions.

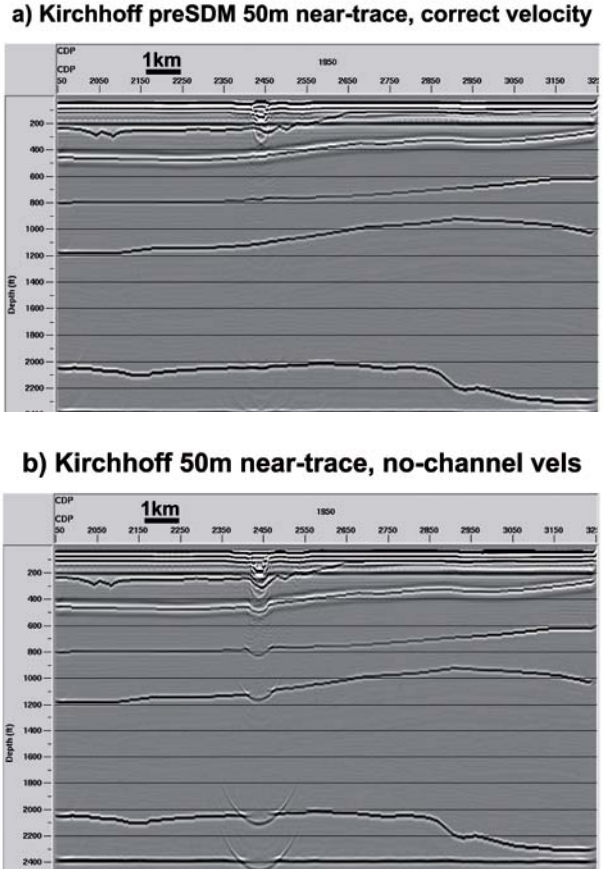

Figure 3 (a) Near-trace section from the Kirchhoff PreSDM using the correct velocity model shown in Figure 1. (b) Near-trace section from the Kirchhoff PreSDM using a velocity model without the channel feature. The push-down image distortion is clear throughout the migrated section.

channel feature produces the expected push-down image distortion in the migration (Figure 3b). In these figures I show the near-trace (50 m source–receiver offset) migrated results, rather than the stacks, as they emphasize the effects we are discussing.

A muted stack of the PreSDM migration (Figure 4), produced using a migration model with no channel anomaly in the velocity field, clearly shows the extent of channel imprints on the migrated image. The lateral extent of the near-surface channel imprint far exceeds the width of the channel itself. The maximum lateral extent of the distortion covers over half a cable length on either side of the near surface anomaly itself (Armstrong et al., 2001), as indicated in the raypath lines for the cable length used in the stack in Figure 4. The total width of the affected zone decreases towards the surface due to the effect of the mute restricting the maximum effective offset in the shallower parts of the stacked section. At depth, the affected zone reaches a maximum width approximately equal to the anomaly width, plus the cable length, plus the Fresnel zone diameter. Here the channel is about 500 m wide and its post-migration Fresnel width is about 60 m. A detailed analysis of this phenomenon was given by Armstrong et al. (2001).

An important detail related to unresolved short scale-length anomalies can be noted from the two inset gathers in Figure 5, where I show a zoom on the reflector at 2 km depth for a near-offset section and the muted stack for the Kirchhoff PreSDM using the no-channel velocity model. Following migration, or moveout correction, the residual moveout in the gather should be approximately parabolic if all the traces in the CMP encountered a similar velocity distribution along their raypaths. When this is not the case, we see 'kinks' in the residual moveout behaviour. This tell-tale behaviour is a clear indication that we have an unresolved anomaly of short scale length somewhere in the overburden. These anomalies can only be resolved by using PreSDM with an appropriate velocity model. Figure 5c indicates how the distortion due to the unresolved channel changes offset position in the gather, for different surface locations.

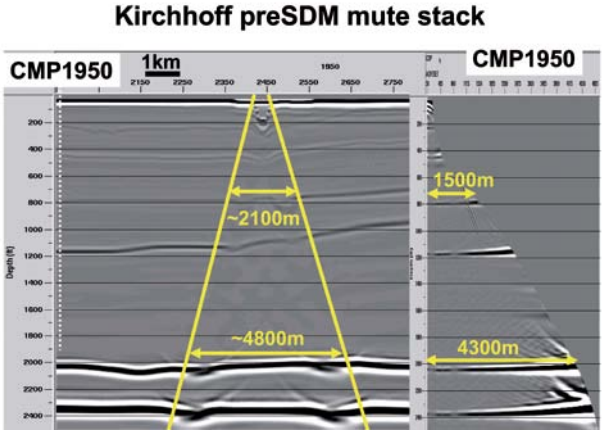

Figure 4 *Stacked section for a maximum offset of 5 km following PreSDM using a velocity model without the channel feature. The inset gather indicates the available offset range with depth, after muting. The image distortion has a lateral extent related to the available offset range: the arrows indicate the post-mute maximum effective offset contributing to the stack, and show why the narrow channel can distort the image over such a wide area.*

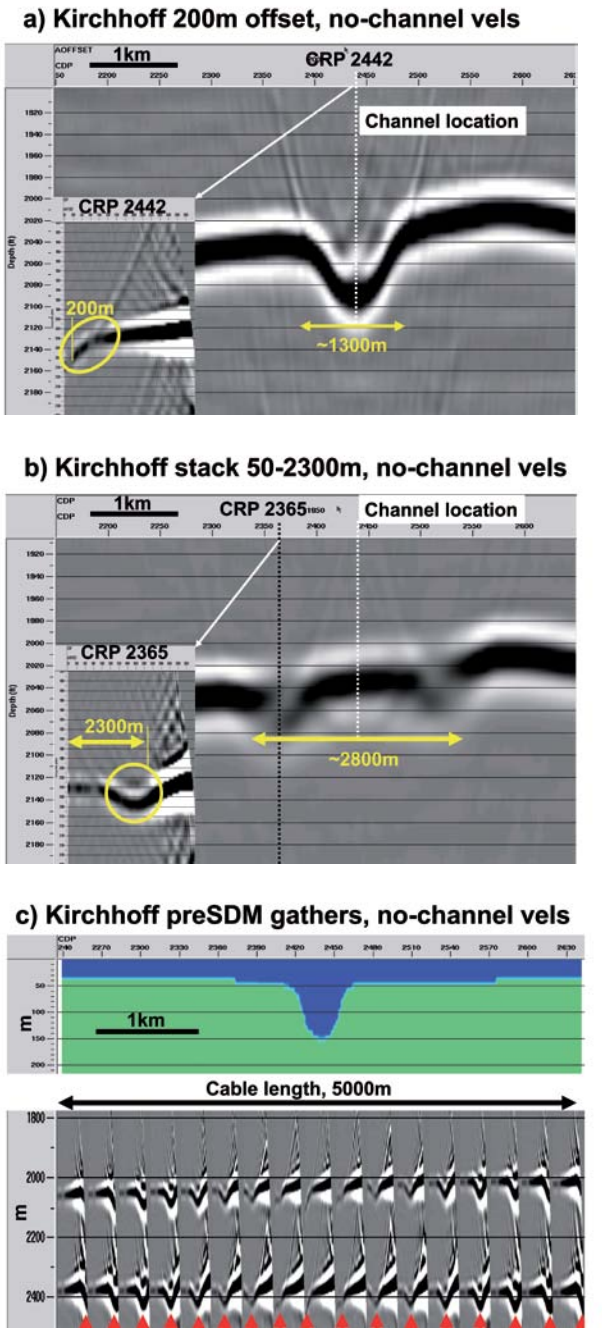

Figure 5 *(a) Zoom on the 200 m offset section from the PreSDM with the smooth velocity model. A CRP gather from the centre of the channel is inset: the near traces in the gather are pushed down as expected (indicated by the circle). (b) Zoom on a limited offset stacked section from the PreSDM with the smooth velocity model. A CRP gather ~1 km distant from the channel is inset – the near traces in the gather are unperturbed and the far-offset raypaths are distorted (indicated by the circle). (c) Selection of gathers, showing how the distortion caused by the channel changes location with offset for different CRP locations (indicated by the red arrows).*

Q: When is a push-down not a push-down?
A: When it is a pull-up!

Counter-intuitively, sometimes the expected push-down effects associated with a low-velocity anomaly can manifest themselves as a pull-up effect on the far offsets of a CMP gather on both NMO-corrected or PreSTM data if the 'correct' velocity model is used. This is because the far-offset raypaths for a CMP location over the channel feature, which do not encounter the channel anomaly because they undershoot it, are treated in the NMO or PreSTM with the single velocity function pertaining to the CMP location of the channel feature. Hence the far-offset traces are processed with a velocity too low compared to the velocity the raypath actually encountered. In other words, both NMO and PreSTM treat all traces within the ray bundle of the CMP gather as if they propagated in a 1D earth model containing the anomaly. Figure 6a is a zoom on the velocity model to show which portions of the far-offset raypaths are being mishandled.

Figure 6b shows the 3050 m offset plane from the data after NMO using the 'correct' velocity model, namely that used to create the data, with an NMO-corrected gather from the centre of the channel shown on the right. The unexpected pull-up on reflectors below the channel, which is seen as an overcorrected curl-up on events in the CMP gather, is due to the far offsets being treated as if they propagated through the channel. This counter-intuitive pull-up effect is exacerbated with an increase in the velocity contrast between the channel fill and the surrounding sediment background velocity. For real data, where the velocities are picked using conventional analysis of velocity spectra so as to maximally flatten reflection events in the CMP gather, this effect will not be seen, except as discussed later.

In Figure 7, I show another synthetic example that represents deep water canyons (Jones, 2010). Here a slight synclinal feature, at 2 km depth, or 2.6 s two-way time, below a deep seabed canyon appears as an anticline on the PreSTM image. Again, the gather on the right of the figure shows the distortion of the moveout behaviour in the PreSTM gather which produces this effect, when migrated with the 'correct' velocity model.

These observations underline the fact that there is no such thing as a 'correct' PreSTM velocity model: we can only obtain a compromise between ignoring lateral velocity change, whilst trying to flatten reflection events in a CMP gather.

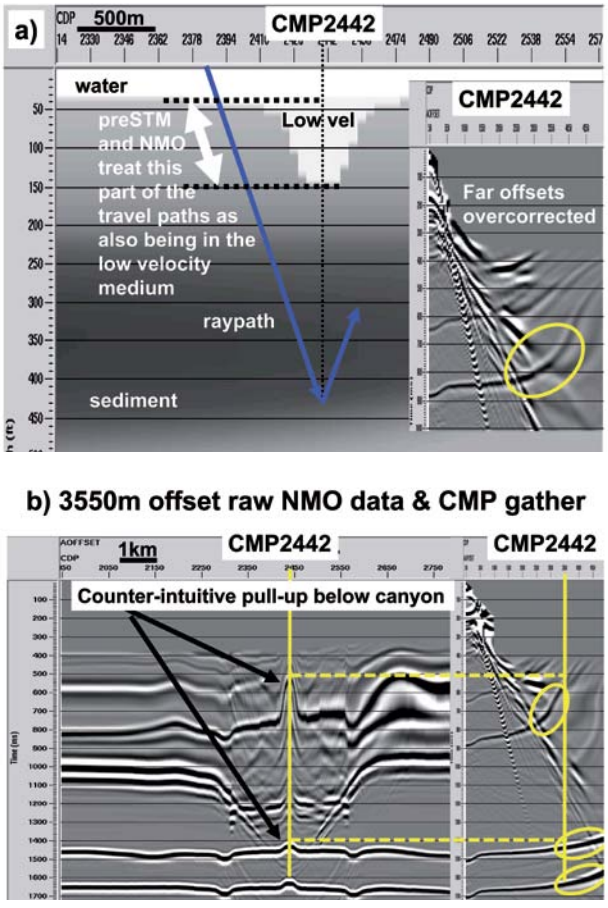

Figure 6 (a) Far-offset raypath at CMP location over channel does not encounter the channel, but is NMO corrected using the channel velocity. (b) NMO overcorrects the far-offset trace, as the low velocity is involved in the correction.

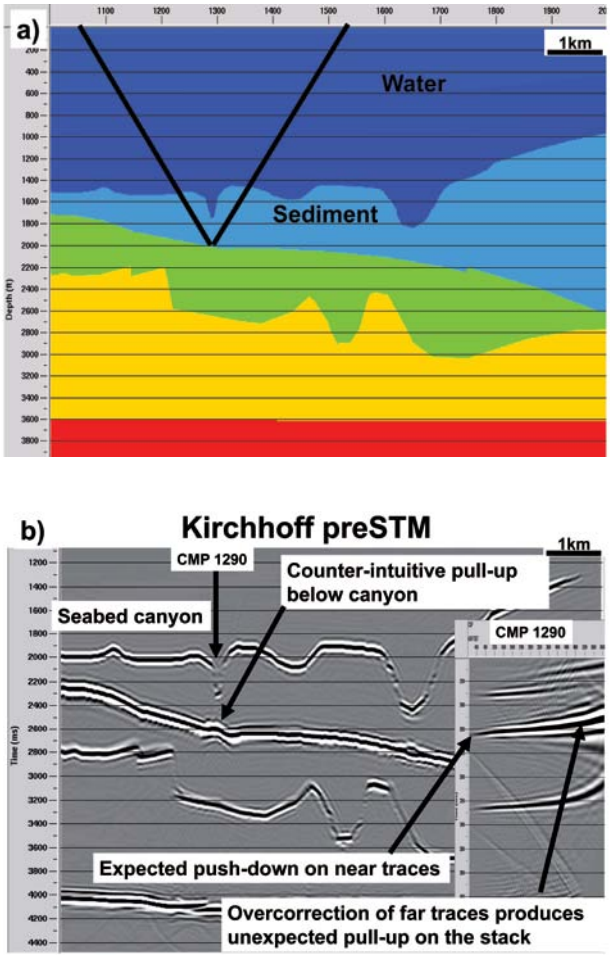

Figure 7 (a) Velocity model for deep water synthetic example with seabed canyon. (b) PreSTM image shows counter-intuitive pull-up below the canyon.

The consequence is that image distortion remains below velocity anomalies. The only way to remove such image distortions is by using PreSDM with the appropriate velocity model.

In practice, this effect is seldom, if ever, seen on real data because the heavily distorted far offsets are muted off. Also, and more importantly, the velocity function obtained by conventional velocity analysis is biased by the far-offset raypaths so as to produce a flatter response on the far traces in the NMO-corrected, or time-migrated, CMP gather, with a consequent slight push-down in the moveout behaviour of the mid-offset traces in the gather. This effect is sometimes seen in an image as a 'wobble' on otherwise flat horizons, when velocity analysis has been performed over a short offset range, but the data have then been stacked using a longer offset range. In addition, refraction at the flanks of the channel, which may be steep, adds to the raypath distortion, tending to broaden the deeper imprint for a low velocity anomaly.

Such raypath distortions resulting from localized heterogeneity can be confused with anisotropic behaviour. Although, in some sense, all anisotropy could be described as resulting from heterogeneity, the effects we are reviewing here are velocity changes on a scale length less than the acquisition spread length, but large enough to be readily included in the velocity model. A rule-of-thumb for distinguishing between this class of heterogeneity and anisotropy is the rapidly varying and inconsistent behaviour of the phenomenon when it results from heterogeneity. If the observed effect was a result of real anisotropy, there would be some spatial consistency in its higher order moveout behaviour.

Land environments: topography and statics

When processing land data, it is important at all stages of the processing to know what datum is being used: is it the acquisition surface, or a near-surface floating datum (smooth version of the true elevation in time or depth), or a locally flat CMP processing datum, or the final flat datum to which the migration velocity model is referenced? I will first review the reasons for introducing these various datums, defining the static shifts involved in moving to them, and then note which should be retained for pre-stack imaging.

For land data, there are several factors that introduce travel-time distortions to what would otherwise be smooth moveout trajectories in gathers. Rapidly varying elevation introduces trace-to-trace jitter, as do near-surface velocity variations due to such things as weathered zones, karstic voids, and dunes. In addition, if the surface is not horizontal, then even for a constant-velocity medium, the moveout behaviour in CMP gathers is not hyperbolic, so velocity analysis and other 2D transform-based processes such as Radon and *tau–p* filters are compromised. Hence for conventional data pre-processing and NMO velocity analysis we have to apply various static corrections at the source and receiver, which are typically surface-consistent, and at CMP locations, in an attempt to make moveout behaviour look locally more hyperbolic. In other words, a 'static' is a time shift applied to a trace to accommodate either a shift from its true surface elevation to some processing datum level (e.g., Zhu, et al., 1992; Cox, 1999), or a travel-time distortion resulting from an unresolved velocity anomaly.

Figure 8 summarizes the different sources of statics for a land environment. In the marine environment we can also have static effects between sail lines, related to tidal and temperature variations, that need to be dealt with during processing. On the left of the figure, we note a floating datum specific to each individual CMP gather (the blue line in Figure 8). This is locally flat within the CMP, and is designed to make moveout behaviour look locally hyperbolic within each CMP gather once the traces are moved to this floating datum. The near-surface model static for each trace in a CMP is made up of high spatial frequency (HF) surface-consistent components at both the source and receiver locations, which result from any rapid topographic variations and any rapid near-surface velocity variation, plus a low spatial frequency (LF) CMP-consistent component to shift all traces in the CMP from their shot and receiver elevations to a common flat processing datum at the CMP elevation. For near-surface velocity variation, i.e., the weathered zone, we typically shift traces to the base of the weathered zone with the weathering velocity, and then back to the surface with a replacement velocity. These shifts might not be truly surface-consistent if the anomalous zone is at some distance from the surface. When the HF and LF statics have been applied there may still be some very high spatial frequency jitter (VHF) which can be removed using residual static techniques.

Finally, for convenience, it is preferable to have all traces output from the processing to be of the same length, referenced to a common origin; hence times will be referenced to an overall flat datum. During pre-processing, this might be an intermediate flat datum at some average elevation, but for migration it will often be a final flat velocity datum plane situated above the highest point of the topography, with a constant replacement velocity between it and the near-surface floating datum, which is a smooth version of the actual topography. Figure 8 shows these datum surfaces. Hence there are two elements of the LF static correction: one designed for processing of CMP gathers, and one to make times relative to a final flat velocity datum. The total model static is the sum of all the HF and LF components.

However, for pre-stack migration, where we are able to either ray-trace or downward-continue from the near-surface floating datum, we do not in general want to apply all of these static corrections because they would themselves introduce near-surface image distortions. The statics we may still want to apply for pre-stack migration, in both time and depth, depend on the lateral scale length of the near-surface velocity anomalies. If, for example, the near-surface velocity anomalies are smooth enough to be properly handled by the migration, then we should incorporate them in the migration

velocity model, and not as static corrections. And, if the surface topography is smooth on a scale length comparable to the travel-time sampling for ray-based methods, say 200 m, we would not require a statics correction for topography but could migrate the data as they stand. If, however, the topography varied rapidly, and/or we were unable to incorporate near-surface velocity anomalies into the velocity model, then a static treatment would still be required to shift the data to the smooth near surface datum (the black dashed line in Figure 8).

Whereas time migration cannot, by definition, deal with lateral short-wavelength velocity anomalies of less than a cable length in width, depth migration should be able to do so, provided the anomaly is large enough to be resolved by the model building procedure, and smooth enough for ray-tracing to honour it if we are using a ray-based scheme such as Kirchhoff or beam migration. That still leaves very small-scale velocity or topography anomalies that we might need to address with a static solution (indicated with the green arrows in Figure 8). In addition, all traces output will be referenced to the flat velocity datum: the LF static for this is added to ray-trace times so it does not bias the velocity estimation. Where these corrections are actually applied in the processing sequence depends on the specific software being used.

If the surface elevations of the shots and receivers are handled correctly then, as with near-surface velocity anomaly effects, there should be no imprint of the topographic relief on the deeper seismic image. So for land data, just as we need to quality control marine data with near-surface channels, we need to ensure that there are no remnant pull-up or push-down distortions on the deeper parts of the image that resemble the surface topography. Ways of performing this quality control include creating a map of the arrival times or RMS amplitude distribution on a deep horizon and comparing them to the near-surface features, such as topography and/or channel distributions, to highlight any remnant imprints on the image.

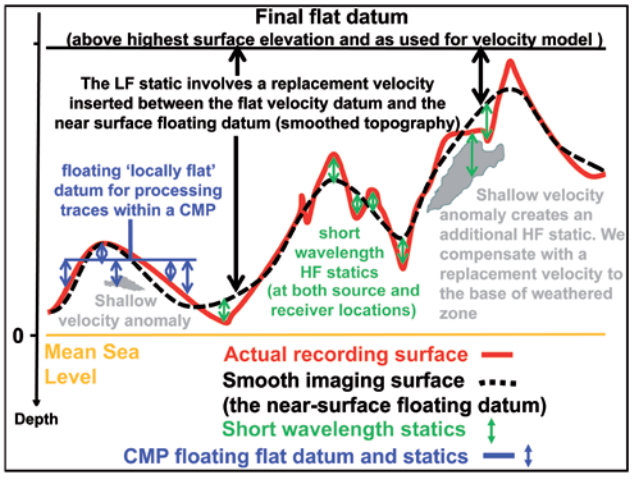

Figure 8 *Different sources of statics for land data.*

Methods for estimating geobody velocity structure

In the following examples, I have divided the methods reviewed into the following sub-groups:

1) When we have sufficient fold of coverage in CMP gathers at the base of shallow anomaly and are thus able to measure velocity error associated with the geobody.
2) When we can only see the base of the geobody on a stacked section, but due to low fold of coverage or noise, are not able measure its velocity error in CMP gathers.
3) When we cannot see a clear stacked image, nor see events on a gather, but can still measure deeper geometrical distortion caused by the shallower geobody (pull-up or push-down).
4) Refraction analysis.
5) Waveform inversion, with a brief mention of surface wave (ground roll) analysis.

It is also important to consider how to preserve any small-scale detail introduced into a velocity model during successive iterations of model update. In general, an iteration of ray-based tomography only updates velocity in the tomography cell as a single perturbation value, added or subtracted to the existing values of velocity in that cell. These cells are typically about 400 m × 400 m × 200 m in size; consequently, the geometry of features of size comparable to these dimensions is unlikely to be altered much in a subsequent iteration of tomographic update (Lo and Inderwiesen, 1994). Furthermore, current industrial practice sidesteps the problem by introducing constraint layers, above which successive tomographic iterations are not permitted to alter the model, a technique often referred to as hybrid gridded tomography (Jones et al., 2007).

Method 1: measurable velocity error on CMP gathers and use of conventional tomography

In the best-case scenario, we can see the anomalous geobody feature on a stack, and there is discernible moveout in the gathers related to the velocity anomaly. In other words, we can pick the velocity error. In this case, we might be able to tomographically invert to resolve the velocity anomaly (Kosloff et al., 1996). However, using ray-based techniques (Bishop et al., 1985) does face the limitation of the high-frequency approximation, so we would not be able to correctly resolve and invert for geobodies whose spatial extent is similar to the wavelength of the seismic waves illuminating them (Worthington, 1984; Pratt et al., 2002; Pratt, 2003; Jones, 2010).

Figure 9a shows the 3D PreSDM image from a North Sea data example with a clearly visible near-surface channel that has a high-velocity fill. The channel produces a severe pull-up distortion in the underlying image. Running a dense autopicker, typically picking on CRPs with a 50 m × 50 m spacing following an initial PreSDM with a smooth starting model, and then updating the velocity with constrained

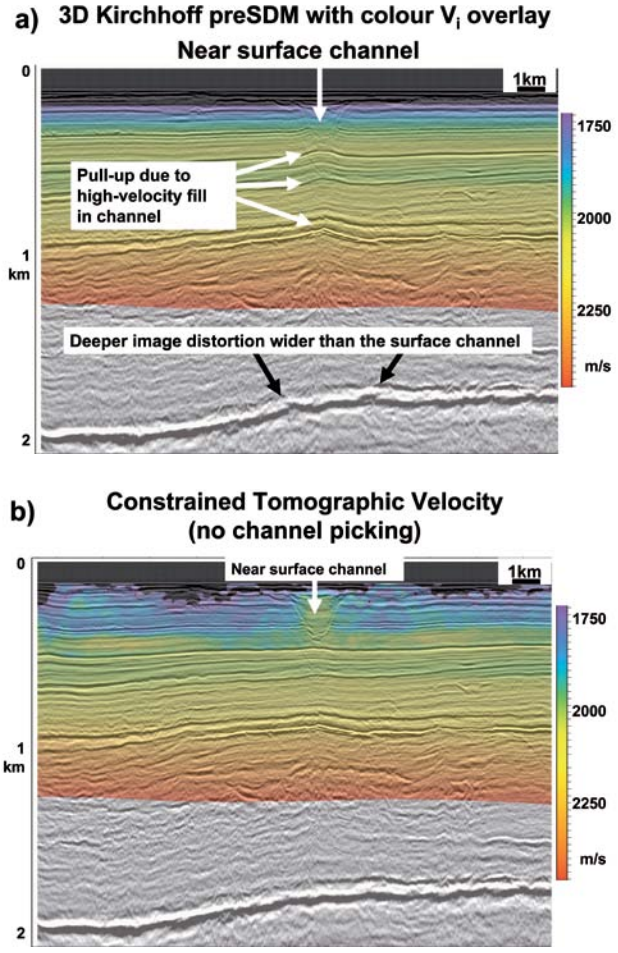

Figure 9 *(a) PreSDM image showing a shallow channel with high-velocity fill causing pull-up distortion in the image. (b) Moveout at the base of the channel was discernible on the CRP gathers, so could be picked to allow tomographic inversion to partly resolve the velocity anomaly and remove most of the deeper image distortion.*

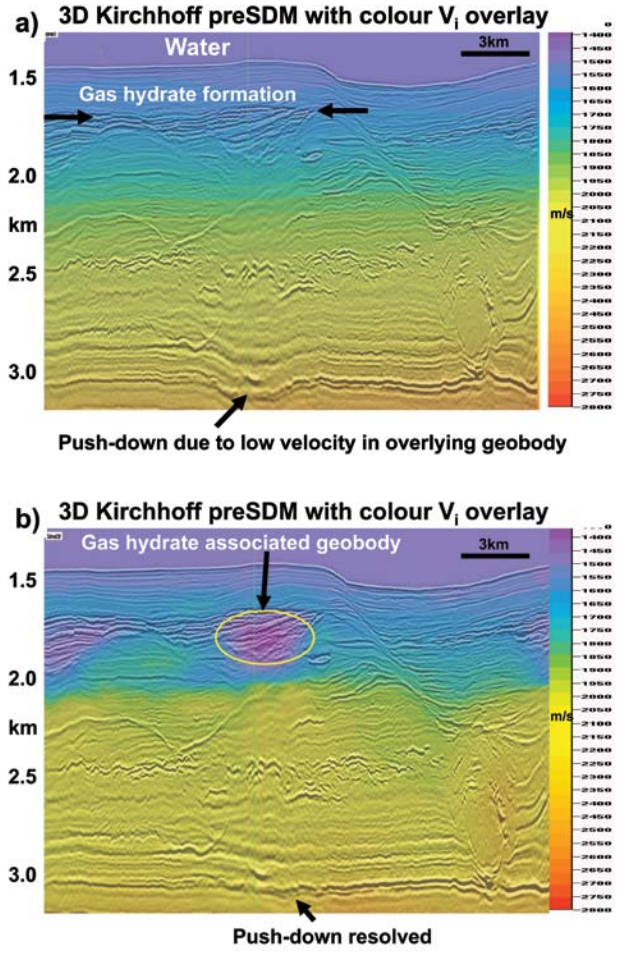

Figure 10 *(a) A low-velocity anomaly associated with a deep water gas hydrate cap results in push-down image distortion in the deeper section. (b) Automated picking of residual velocity error on the CRP gathers permits the tomography to update the model well enough for the push-down to be mostly resolved (from Fruehn et al., 2008; courtesy of Reliance Industries).*

high-resolution gridded tomography mostly resolves the pull-up artefacts and improves the deeper PreSDM image (Figure 9b). However, allowing the tomography to introduce such a rapid velocity change in the model can result in instabilities in other parts of the updated velocity field, so great care must be taken to restrict the rapid velocity changes to those parts of the model where we know there to be anomalies.

In Figure 10a, the second example, from offshore India, shows a low velocity anomaly below a possible gas hydrate formation (Fruehn et al., 2008). Sometimes these anomalies are due to gas build-up which can pose a serious drilling risk because of the potential for overpressure, and sometimes they are due to high porosity sand/shale units with normally pressured gas. Employing high resolution tomography following PreSDM can help to identify these geobodies – of use both in avoiding drilling hazards and also in highlighting potential hydrocarbon reserves. Again, dense autopicking followed by tomography has resolved the low velocity geobody, and compensated for most of the deeper push-down image distortion on the 3D PreSDM (Figure 10b).

Method 2: discernible geobody geometry

In a scenario where we have poor data quality, perhaps due to low fold, where we are unable to pick moveout in gathers, so have no direct way to estimate velocity error, but are still able to pick the base and top of the geobody on a stack, we can proceed using a trial velocity within the geobody. The trial velocity might be estimated from assessing deeper pull-up or push-down, or simply be a guess confirmed using a velocity scanning technique.

For intricate narrow channels present in the Mio-Pliocene section just below the seabed in an Indian case study, manual interpretation of the top and base of the channel features was used to define the channel geometry, combined with a scan over potential channel-fill velocities. The channels were picked on a dense localized grid of inlines and crosslines. The 3D PreSDM image in Figure 11a shows 1500 m of data below the seabed, where we see deeply incised seabed canyons, but also some small localized buried palaeochannels just below the seabed. These channels result in a severe push-down distortion of the underlying sediments due to their low velocity fill.

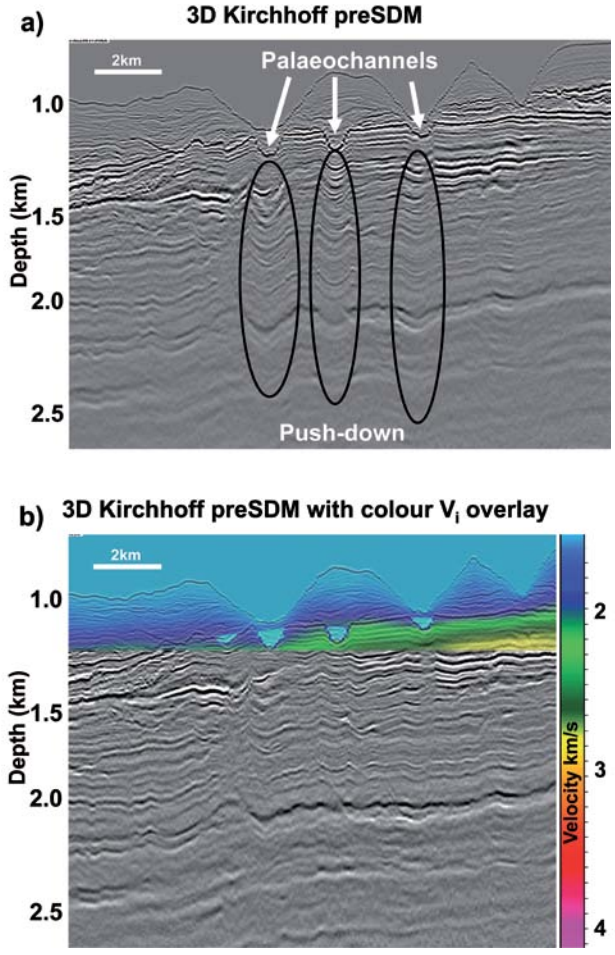

Figure 11 (a) Deep water buried palaeochannel near the seabed, with low-velocity fill, causes push-down image distortion. (b) Detailed manual picking of these geobodies, in conjunction with a reasonable trial velocity in the channels, helps resolve the image distortion (from Fruehn et al., 2008; courtesy of Reliance Industries).

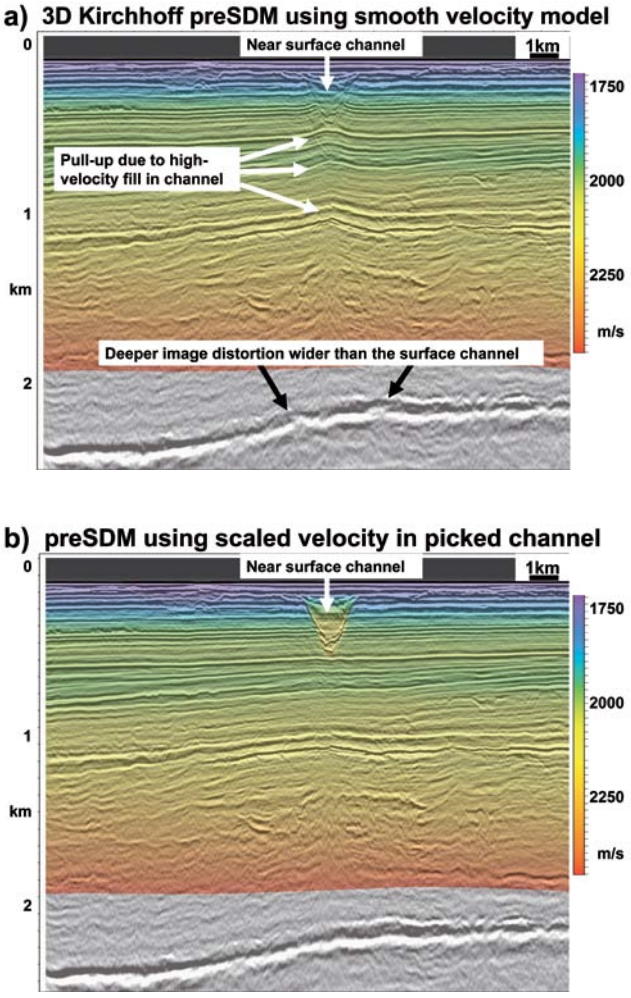

Figure 12 (a) Shallow water high-velocity channel causing pull-up. (b) Manual picking of the channel and a reasonable trial velocity helps resolve the laterally widespread deeper image distortion.

If we were to use a smooth velocity model, or perform imaging using PreSTM, we would be unable to resolve these small-scale features, which are typically 300–400 m in width. The 3D PreSDM image of Figure 11a was created using a smooth background velocity field; hence the push-down is visible. Following a migration velocity scan to determine the best channel-fill interval velocity, a PreSDM using the channel-fill model was performed (Figure 11b). The velocity model is overlaid in the shallow part of the section, indicating the low velocity channels. The improvement in the deeper section, below about 2 km depth, is significant: we have not perfectly resolved the shallow channel problems, but incorporating them in this way enables better resolution in the deeper section. Ignoring them is not a viable option.

Using the same North Sea data as shown in Figure 9, the trial velocity approach is also demonstrated. The 3D PreSDM image in Figure 12a shows those data after some further wavelet processing, hence the different phase, compared to Figure 12b which shows the PreSDM results after picking the geobody and inserting a trial velocity. This method, too, has resolved the push-down in the deeper section, giving a comparable result to that of the tomographic technique shown in Figure 9b.

The trial velocities can be obtained either from an initial tomographic estimate or from analysis of distortion on deeper events, and combined with a migration scan to select an optimum velocity. However, resorting to manual picking always tends to slow down a project; hence from a turnaround-time perspective we try to avoid manual intervention unless we have no option.

Method 3: deeper geometric distortion

In very shallow water, the ringing seabed multiples and direct arrival often obscure near-surface channels, making it difficult to either pick the features on an image or discern moveout behaviour in the low fold data. In Figure 13a, one such example from the North Sea is shown. The channel is not visible in the 3D PreSDM images, but the push-down distortion of deeper layers is. In this particular case, some high resolution 2D data were available, so typical channel geometries were estimated from this grid of 2D data.

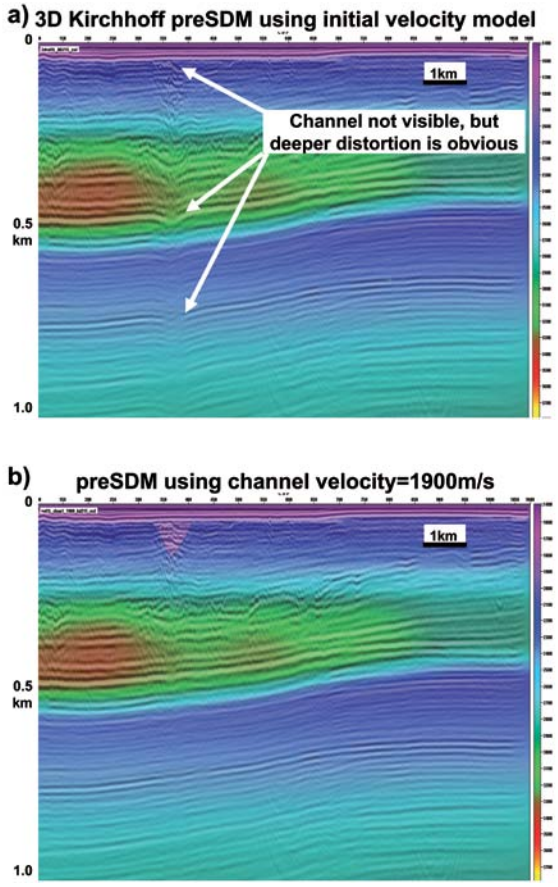

Figure 13 *(a) Shallow water low-velocity channel causing push-down visible in the deeper section. (b) The channel itself is not visible, so picking of a distorted deeper event permits an estimation of the trial velocity to help resolve the deeper image distortion (courtesy of Hansa Hydrocarbons).*

More generally for this type of 3D data, the geometry and fill velocity of the channel features would be derived by mapping the channel imprint on a deeper reflector. The imprint effect is estimated by subtracting a smoothed and unsmoothed surface, picked on a PreSDM image created using a smooth background velocity model, without any channel features. These residuals are then smoothed to remove very high-frequency effects and/or empty bins, converted to time using the smooth migration velocity model, and converted back to depth using a trial channel velocity.

The channel feature is adjusted by vertically stretching the geobody derived from the residuals, such that in conjunction with the trial velocity, the deeper imprint is removed. In this case, the channel width was assumed to be somewhat narrower than the imprint, with the channel situated just below the seabed. Remigrating with the modified model, after some refinements, produced the result in Figure 13b: the deep distortions have been mostly removed.

Method 4: refraction tomography

Various refraction techniques are available for determining a near-surface statics model, which in turn can sometimes be of use to estimate a near-surface velocity model. These methods normally involve picking the first breaks on shot records, deriving a spatially variant velocity model along a variable number of refractor surfaces, and computing time delays through the resultant weathering model. A more complete and complex near-surface velocity model can be obtained by using a gridded tomographic procedure. Here I show results from one such 3D tomographic velocity inversion procedure that uses turning (diving) rays to iteratively solve for velocity anomalies in the near surface (Cunningham, 2008). However, as the refracted raypaths may take a more horizontal route through the subsurface than reflected seismic data, we must ensure that the velocity model we are building is anisotropic so as to accommodate the directional dependence of velocity. It may also be possible that the velocities estimated from the more horizontal raypaths differ from those estimated from reflection data due to unresolved anisotropic and other effects in the near surface.

As part of calculating tomographic statics, it is important to limit the surface model update to only that part of the subsurface encompassed by the diving raypaths, as it is these arrivals, appearing as refraction events on the shot records, that the tomography will use. This sets a limit on the depth of the weathering model we can obtain. The depth limit can be chosen by analysing the raypath hit count map to see

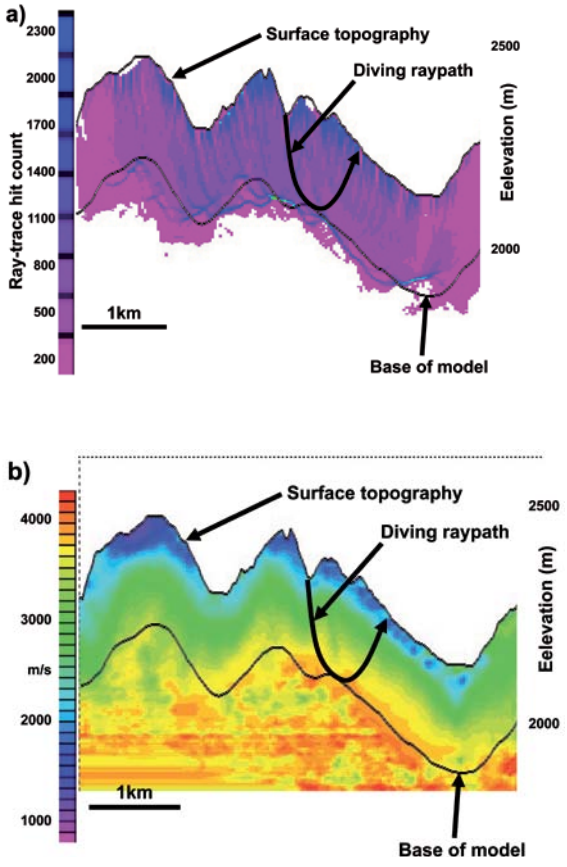

Figure 14 *(a) Ray-trace hit count for turning raypaths. (b) Tomographic inversion of turning rays, indicating low-velocity anomalies near the surface (from Cunningham, 2008).*

where we have valid ray coverage. One method for selecting the base of the weathering model is to smooth the surface elevations and subtract a constant depth from the smoothed surface elevations, while making sure that the base of the model is not deeper than the area where we have valid ray-path coverage. Figure 14a shows the ray-trace hit count for a line through a 3D land example. The model update is limited to about 250 m below the surface, and the tomographic solution (Figure 14b) indicates various low-velocity anomalous zones very close to the surface.

Method 5: waveform inversion

The methods outlined so far have been mostly empirical, based on some seriously limiting assumptions, and in general produce very approximate solutions. To move beyond these crude methods, we need a technique that can better estimate the small-scale velocity distribution of the near surface, and waveform inversion is intended to do this. Waveform inversion, also referred to as waveform tomography or full waveform inversion (FWI), has the potential to deliver accurate and precise estimates of near-surface velocity structure at a scale length similar to the wavelength of the seismic waves being recorded. More conventional ray-based tomographic techniques are limited in their resolving power to several times the wavelength of the recorded waves.

Whereas ray-based tomography relies on measuring only the arrival time or depth of reflection events as seen in a gather, waveform inversion uses the amplitude and phase, and hence arrival times as well, of the reflection and/or transmitted arrivals in the data. At the heart of the procedure is a forward modelling process that attempts to reproduce the observed, real seismic data. Hence, to assess its usefulness and validity, we need to question how well the process accurately deals with amplitude behaviour (Warner et al., 2010). Below I list several topics that are intimately related to the amplitude of modelled data:

- *Elasticity, addressing shear modes.*
- *Viscosity, incorporating attenuation, Q.*
- *Anisotropy, addressing the directional dependence of velocity.*
- *Acoustic wave propagation – P-wave only, thus ignoring density variation.*
- *Source wavelet, including ghost effects.*
- *Source wavelet time delay.*
- *Cycle skipping, with offset and frequency dependence.*

Approximations and errors in dealing with any of these items compromise our ability to accurately model the observed seismic shot gather; hence it is instructive to assess each of these items in turn.

To model 3D data with a full orthorhombic anisotropic visco-elastic representation of the wave equation is very expensive and requires estimates of a 3D model for density, P-wave velocity, S-wave velocity, Q, tilted transverse isotropy (i.e., TTI anisotropy), and azimuthal anisotropy parameters. This representation is beyond the current state of the art; hence most implementations being showcased in the industry today use an acoustic approximation, i.e., treating all solids as liquids, ignoring mode conversion and S-wave propagation. A consequence of this approximation is that, for big reflection coefficients such as at the seabed, we have a large error. The error arises because for the real data, a significant portion of the incident energy is converted to shear waves, resulting in smaller amplitudes of the P-wave arrivals; hence the modelled amplitudes are incorrect. Likewise, ignoring absorption leads to overestimation of amplitudes in the modelled data. Some algorithms at least attempt to address density variation, attenuation, and TTI anisotropy, by using a priori values for these parameters in the forward modelling; in other words, we do not try to invert for them, but assume we know them well enough to begin with, and supply a model of them to the algorithm.

If the errors in reflection coefficients arising from the acoustic approximation are considered too large, then we can rely on transmitted energy (refractions, turning or diving rays) to drive the inversion. However, using this restriction means that we either must use very long offset data, or restrict the depth of the inversion to about one third of the cable length, a rule of thumb for the depth of penetration for diving waves.

Knowing what source wavelet and phase to use in the forward modelling is also important. This is non-trivial if we are using a time domain modelling routine, as the recorded waveform in real marine data has embedded in it the source and receiver ghosts, as well as the bubble pulse. Hence the modelling must take account of what wavelet estimate we have when the boundary conditions in the forward propagator are set, i.e., should we include a surface-bounce ghost in our modelling to match what is in the recorded data, or have we already removed these ghosts from the real data in some pre-processing step, and thus do not want to create them in the modelled data?

The source delay relates to the question of where time zero is in the real and the modelled data. Most marine sources comprise an airgun array, so the origin time of the wavelet varies as a function of azimuth and take-off angle, and hence will be different for all offsets. Also, if we have a complex high-bandwidth wavelet, then even for a small initial error in a starting model, we may get cycle skipping between the real and modelled data on the far traces, and obtain a misleading local minimum in the inversion result giving rise to an incorrect velocity model update (Bunks et al., 1995). To help avoid the cycle skipping and local minima problems, the starting model for FWI needs to be good, and is typically the result of a few iterations of conventional ray-based tomography. Hence, the state of the art, at least for data domain waveform inversion, tends to rely on long offsets, low frequencies, and to a large degree, turning wave data (Plessix and Perkins, 2009; Vigh et al., 2009; Sirgue et al., 2010; Wang et al., 2011).

Figure 15a shows a depth slice through a velocity model derived from conventional tomography for a Caspian Sea

example (Sirgue et al., 2011). Figure 15b demonstrates the increase in resolution achievable with FWI as compared to conventional ray-based technique: in this case, shallow gas-charged anomalies are much better resolved, leading to enhanced imaging of the deeper section.

A technique of increasing interest is surface wave inversion. Here, the high amplitude groundroll events that plague land and OBC data recordings are themselves exploited in an attempt to estimate near-surface properties, primarily shear velocities. By analysing the dispersion behaviour for various propagation modes, S-wave velocity estimates can be obtained for the first few hundred metres below the surface. For the ground-air interface, Rayleigh waves yield the SV velocity, and Love waves yield the SH velocity, and for the seabed-water interface Schulte waves also yield the SV velocity (e.g., Socco et al., 2010; Douma and Haney, 2011; Haney and Douma, 2011).

Conclusions

Resolution of near-surface velocity anomalies remains a difficult problem. Failure to resolve such anomalies severely restricts our ability to adequately image deeper geological structure; hence some form of solution to the problem is imperative.

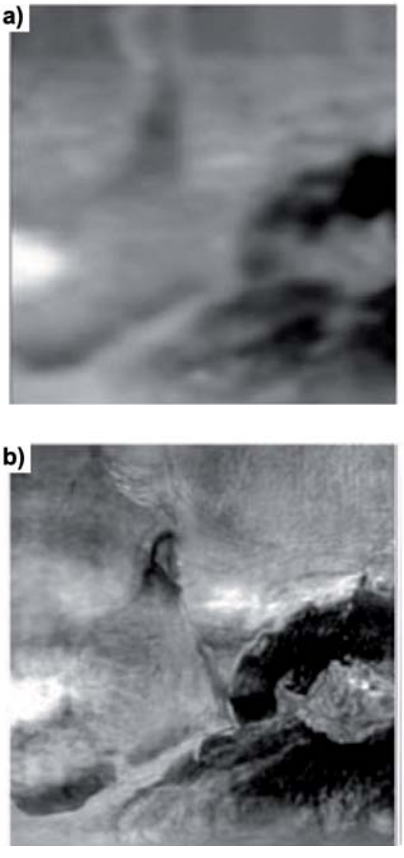

Figure 15 *(a) Caspian Sea example showing velocity model shallow depth slice obtained using conventional ray-based tomography. (b) Corresponding FWI result. (Courtesy of Total).*

A range of sub-optimal bespoke techniques is available, but usually involve painstaking and time-consuming effort. For the most part, the automatic pickers used to provide residual moveout information for tomography rely on parametric approximations: in other words, they fit a smooth simple curve, such as a parabola, to the residual moveout behaviour of an event across offsets. This imposes an inherent limitation on the resolution of features of small scale length, which can to some extent be circumvented by using non-parametric picking (Brittan and Yuan, 2005). However, reliably picking undulating residual-moveout behaviour is notoriously difficult; hence we have a trade-off between stability of picking and velocity resolution. Even with less restrictive autopickers, the issues outlined in this review still remain, as the fold of coverage for shallow anomalies is often too small to be useable for autopicking.

Fortunately, given sufficient time, the techniques described here commonly do offer the possibility of resolving many of the image distortion problems caused by near-surface velocity anomalies And, looking to the future, the emerging technology of FWI offers great promise in resolving small-scale velocity anomalies, but is as yet some way off as a routine full-scale solution for all commercial imaging projects. Hence, until such a panacea is readily available, we need to rely on techniques such as those outlined here.

Acknowledgements

I thank Laurent Sirgue and Paul Sexton for permission to show the results of Total's in-house FWI; Rabi Bastia and Simon Lunn for permission to show data examples; Juergen Fruehn and Mick Sugrue for the PreSDM examples; and Dave Cunningham for the refraction tomography example. I also thank Mac Al-Chalabi, Glenn Morley, Laurent Sirgue, Juergen Fruehn, Mike Goodwin, Ivan Berranger, and Robert Bloor for their help in preparing the manuscript.

References

Armstrong, T. [2001] Velocity anomalies and depth conversion – drilling success on Nelson Field, Central North Sea. *63rd EAGE Conference & Exhibition*, Extended Abstracts, IV-2.

Armstrong, T.L., McAteer, J. and Connolly, P. [2001] Removal of overburden velocity anomaly effects for depth conversion. *Geophysical Prospecting*, **49**, 79–99.

Bishop, T.N., Bube, K.P., Cutler, R.T., Langan, R.T., Love, P.L., Resnick, J.R., Shuey, R.T., Spindler, D.A. and Wyld, H.W. [1985] Tomographic determination of velocity and depth in laterally varying media. *Geophysics*, **50**, 903–923.

Brittan, J. and Yuan, J. [2005] Dense multi-offset reflection tomography. *75th SEG Annual Meeting*, Expanded Abstracts, **24**, 2534–2537.

Bunks, C., Saleck, F.M., Zaleski, S. and Chavent, G. [1995] Multiscale seismic waveform inversion. *Geophysics*, **60**, 1457–1473.

Cox, M. [1999] *Static Corrections for Seismic Reflection Surveys*. SEG, Tulsa.

Cunningham, D. [2008] Millennium: a refraction statics solution. http://www.iongeo.com/content/includes/docManager/Millennium.pdf

Douma, H. and Haney, M. [2011] Surface-wave inversion for near-surface shear-wave velocity estimation at Coronation field. *81st SEG Annual Meeting*, Expanded Abstracts, **30**, 1411–1415.

Fruehn, J.K., Jones, I.F., Valler, V., Sangvai, P., Biswal, A. and Mathur, M. [2008] Resolving near-seabed velocity anomalies: deep water offshore eastern India. *Geophysics*, **73**, VE235–VE241.

Haney, M. and Douma, H. [2011] Inversion of Love wave phase velocity, group velocity and shear stress ratio using finite elements. *81st SEG Annual Meeting*, Expanded Abstracts, **30**, 2512–2516.

Jones, I.F., Sugrue, M.J. Hardy, P.B. [2007] Hybrid gridded tomography. *First Break*, **25**(4), 15–21.

Jones, I.F. [2010] *An Introduction to Velocity Model Building*. EAGE, Houten.

Kosloff, D., Sherwood, J., Koren, Z., Machet, E. and Falkovitz, Y. [1996] Velocity and interface depth determination by tomography of depth migrated gathers. *Geophysics*, 61, 1511–1523.

Lo, T.W. and Inderwiesen, P. [1994] *Fundamentals of Seismic Tomography*. SEG, Tulsa.

Plessix, R.E. and Perkins, C. [2009] 3D full-waveform inversion with a frequency-domain iterative solver. *71st EAGE Conference & Exhibition*, Extended Abstracts, U039.

Pratt, R.G. [2003] Waveform tomography: theory and practice. *12th International Workshop on Controlled-Source Seismology*, Mountain Lake, Virginia. http://geol.queensu.ca/people/pratt/prattccss.pdf

Pratt, R.G., Gao, F., Zelt, C. and Levander, A. [2002] A comparison of ray-based and waveform tomography – implications for migration. *64th EAGE Conference & Exhibition*, Extended Abstracts, B023.

Sirgue, L., Barkved, O.I., Dellinger, J., Etgen, J., Albertin, U. and Kommedal, J.H. [2010] Full waveform inversion: the next leap forward in imaging at Valhall. *First Break*, **28**(4), 65–70.

Sirgue, L., Denel, B. and Gao, F. [2011] Integrating 3D full waveform inversion into depth imaging projects. *81st SEG Annual Meeting*, Expanded Abstracts, **30**, 2354–2358.

Socco, L.V., Foti, S. and Boiero, D. [2010] Surface-wave analysis for building near-surface velocity models – established approaches and new perspectives. *Geophysics*, **75**, A83–A102.

Vigh, D., Starr, E.W. and Kapoor, J. [2009] Developing earth models with full waveform inversion. *The Leading Edge*, **28**, 432–435.

Wang, C., Delome, H., Calderon, C., Yingst, D., Leveille, J., Bloor, R. and Farmer; P. [2011] Practical strategies for waveform inversion. *81st SEG Annual Meeting*, Expanded Abstracts, **30**, 2534–2538.

Warner, M., Umpleby, A., Stekl, I. and Morgan, J. [2010] 3D full-wavefield tomography: imaging beneath heterogeneous overburden. *72nd EAGE Conference & Exhibition*, Extended Abstracts, Workshop 6.

Worthington, M.H. [1984] An introduction to geophysical tomography. *First Break*, **2**(11), 20–26.

Zhu, X., Sixta, D.P. and Angstman, B.G. [1992] Tomostatics; turning-ray tomography + static corrections. *The Leading Edge*, **11**, 15–23.

Received 3 November 2011; accepted 1January 2012.
doi: 10.3997/1365-2397.2011041